INVESTIGATION OF THE MICROSTRUCTURE AND MECHANICAL PROPERTIES OF ELECTRON BEAM WELDED AW2099 ALUMINIUM LITHIUM ALLOY

Miroslav Sahul[1], Martin Sahul[2], Marián Haršáni[3], Milan Marônek[1], Jozef Bárta[1]

[1]Slovak University of Technology in Bratislava, Faculty of Materials Science and Technology in Trnava, Department of Welding and Joining of Materials, J. Bottu 25, 917 24 Trnava, Slovakia

[2]Slovak University of Technology in Bratislava, Faculty of Materials Science and Technology in Trnava, Institute of Materials Science, J. Bottu 25, 917 24 Trnava, Slovakia

[3]Staton, s.r.o., Sadová 1148, 038 53 Turany, Slovakia

Key words: electron beam welding, AW2099 aluminium lithium alloy, equiaxed zone, nanoindentation

Abstract:

Electron beam welding of new generation AW2099 aluminium lithium alloy was performed. The thickness of the experimental material was 4 mm. PZ EZ 30 STU electron beam welding machine was used for production of welds. Maximum accelerating voltage used for welding was 55 kV. Produced welded joints consisted of heat affected zone (HAZ), equiaxed non-dendritic zone (EQZ), columnar dendritic zone (CDZ) and equiaxed dendritic zone (EDZ). EQZ grains were formed due to heterogeneous nucleation on precipitates at the fusion boundary. Nanoindentation measurements revealed, that nanoindentation hardness values were lower in comparison to remaining parts of welded joint. Contrary, Young's modulus was higher for locations in EQZ. Energy dispersive x-ray analysis (EDX) analysis revealed that the interdendritic areas were enriched by alloying elements due to segregation. Higher content of copper was detected in such locations. Fracture occurred in the weld metal due to dissolution of strengthening precipitates caused by welding thermal cycle. Ductile fracture surfaces characterized by the presence of dimples were observed.

1 INTRODUCTION

Aluminium alloys containing lithium have received increasing attention especially in the aerospace industry due to their unique properties such as low density, high strength to weight ratio, high Young's modulus, improved fatigue crack growth resistance and resistance to corrosion as well. Mentioned alloys are therefore counted as possible replacements for conventional 2XXX, 6XXX and 7XXX series of aluminium alloys. It was observed that adding of 1% of lithium resulted in the drop of density by 3 % and rise in Young's modulus by 6 % [1-7].

The third generation of aluminium lithium alloys was developed in order to remove the drawbacks of previous generation. Anisotropy in mechanical properties, low fracture toughness, poor resistance to corrosion, loss of toughness after thermal exposure were the main disadvantages. Among important newly developed alloys belong 2099 and 2199 applied especially in the fuselage's skin stringer components [8]. Al-Li alloys of the new generation are characteristic by higher Cu/Li ratio [9]. The application of 2099 alloy caused the reduction of weight of wing components by 14 % and cryogenic tanks by 21 % [10]. Currently, worldwide research focuses on the welding of aluminium lithium alloys. Friction stir welding belongs to the possible joining methods [11-15].

Fu et al. studied microstructure and mechanical properties of 2A97 aluminium lithium alloy welded by fiber laser. Authors found, that welding defects and loss of strength due to dissolution of precipitates lead to the degradation of mechanical properties. Fracture occurred in the equiaxed zone [16]. Zhang et al. studied the mechanism of the formation of equiaxed grains in welds of 2090 aluminium lithium alloy. Aluminium lithium alloy was fusion welded using several new filler metals containing various amounts of zirconium and lithium [17]. Faraji et al. conducted an investigation on capability of hybrid Nd:YAG laser-TIG welding technology for AA2198 Al-Li alloy [18].

The main issues encountered during fusion welding of these alloys are porosity, hot cracking, loss of alloying elements and decrease in mechanical properties of weld joints. Drop in mechanical properties is associated with the dissolution of strengthening precipitates. From this point of view, the application of low heat input electron beam welding could be more beneficial. Narrower weld metal and HAZ represents softening region of much smaller dimensions in comparison to conventional arc welding processes [19,20].

The aim of the study is to analyse the microstructure and mechanical properties of produced electron beam welds on AW2099 aluminium lithium alloy.

2 EXPERIMENTAL

AW2099 aluminium lithium alloy was proposed as base material. The thickness of 2099 aluminium lithium alloy was 4 mm. Solution heat treatment at 530 °C with holding time of 1 hour and hot rolling was carried out. The chemical composition provided by Smiths High Performance is given in Table 1.

Table 1. The chemical composition of AW 2099 aluminium lithium alloy (in wt. %)

Cu	Li	Zn	Mg	Mn	Zr	Ti	Fe	Si	Be	Al
2.4-3.0	1.6-2.0	0.4-1.0	0.1-0.5	0.1-0.5	0.05-0.12	≤ 0.1	≤ 0.07	≤ 0.05	≤ 0.0001	Bal.

PZ EZ 30 STU electron beam welding machine was used for production of butt welds. The volume of vacuum chamber is 14.3 m^3. The maximum accelerating voltage of the equipment is 60 kV and maximum output power is 30 kW. Maximum accelerating voltage used for welding trials was set to 55.0 kV. The vertical electron beam welding was carried out. The working vacuum was 10^{-2} Pa. Chamber pumping time was 25 min. The focusing current was 885 mA. The heat inputs used for welding of AW2099 aluminium lithium alloy ranged from 44.7 J/mm to 128.3 J/mm.

After metallographic preparation of cross sections, the specimens were etched with Keller's reagent (1 ml HF + 1.5 ml HCl + 2.5 ml HNO_3 + 95 ml distilled H_2O). JEOL 7600 F scanning electron microscope fitted with EDX analyzer X-max 50 mm^2 of Oxford Instruments was used to analyse chemical composition in local sites of weld metal and to observe the fracture surfaces after tensile testing. Anton Paar NHT^2 nanoindentation tester was used for nanoindentation hardness measurements across equiaxed non-dendritic zone and equiaxed dendritic zone of weld metal. Maximum load used for measurements was 10 mN.

3 RESULTS

The dependence of weld bead width, weld root width and cross sectional area is given in Fig. 1. With increasing of the heat input, slight decrease in weld width was observed. The narrowest weld joint was produced with the heat input of 91.6 J/mm. Contrary, cross sectional area of welds increased with the increase of heat input. The lowest values were recorded in the case of heat input 44.7 J/mm. Heat input of 96.3 J/mm resulted in the cross section of 12.36 mm^2. Similar trend was observed in the case of weld root width. The width of the weld root increased with the raise in heat input used. Maximum root width was measured in weld joint fabricated with the heat input of 96.3 J/mm

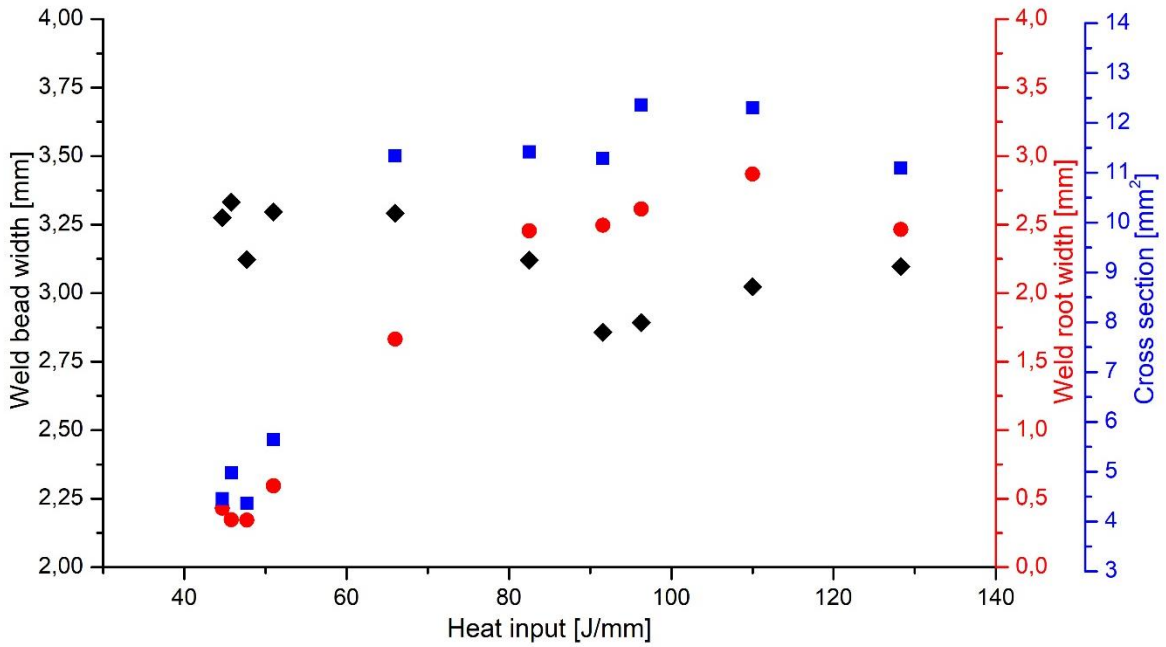

Figure 1. Dependence of weld joint dimensions on heat input used for welding

Microstructure of different zones of weld joint are given in Fig. 2. Weld joints produced on aluminium lithium alloys consisted of heat affected zone (HAZ), partially melted zone (PMZ), equiaxed non-dendritic zone (EQZ), columnar dendritic zone (CDZ) and equiaxed dendritic zone (EDZ) [5]. The width of HAZ is narrow due to low heat input being typical for electron beam welding. Grain morphology varies in the direction from the base metal to the weld centre. The presence of EQZ along the fusion boundary is characteristic for fusion welds on aluminium lithium alloys.

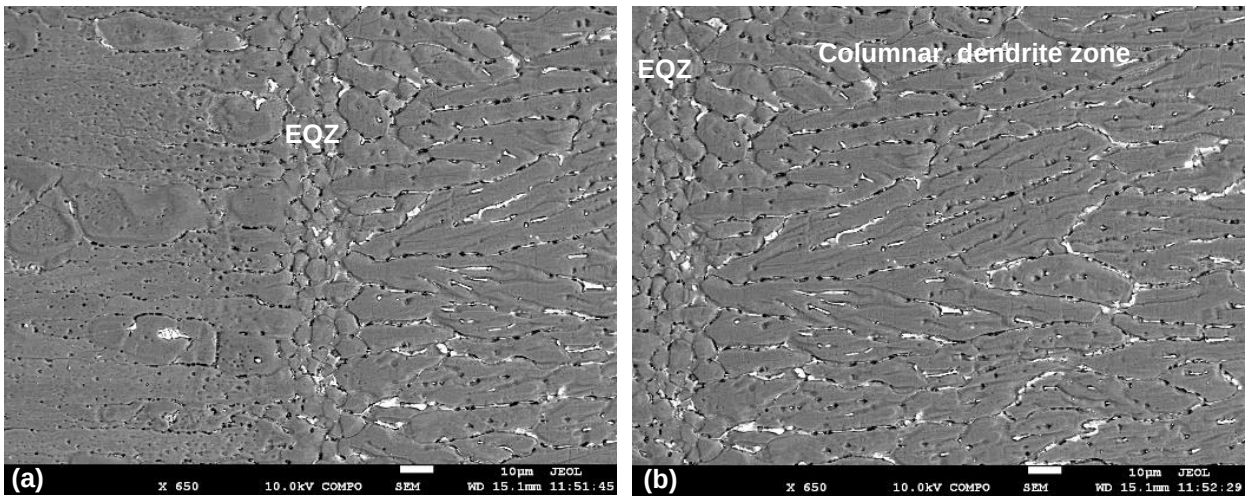

Figure 2. SEM images of selected zones in weld joint: a) AW2099 aluminium lithium alloy – HAZ – weld metal interface, b) Equiaxed non-dendritic and columnar dendritic zone

EDX analysis was performed to analyse chemical composition of various locations in weld metal (Fig. 3). Results of EDX analysis are given in Tab. 2. Spectrums 4, 5 and 8 are characterized by high content of aluminium. More than 98 wt. % of aluminium was measured in mentioned locations. The matrix consists of α-aluminium solid solution. Interdendritic areas are enriched by alloying elements due to segregation. Drop of aluminium content and increase in copper was observed in those areas. Remaining spectrums are brighter, indicating higher content of element with higher atomic number.

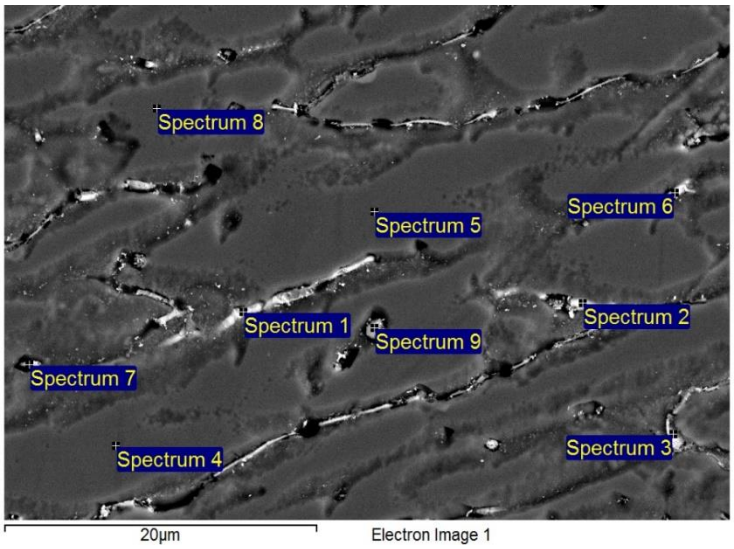

Figure 3. EDX analysis of weld metal

Table 2. Results of EDX analysis carried out in various sites of weld metal

Spectrum	Al	Ti	Fe	Cu
1	58.14	-	-	41.86
2	45.81	-	2.71	51.48
3	64.03	-	-	35.97
4	99.20	-	-	0.80
5	99.08	-	-	0.92
6	50.26	-	1.02	48.72
7	50.89	-	-	49.11
8	98.77	-	-	1.23
9	46.25	-	-	53.75

Fracture surface of weld joint after tensile testing is given in Fig. 4. The ductile fracture characteristic by the presence of dimples was observed.

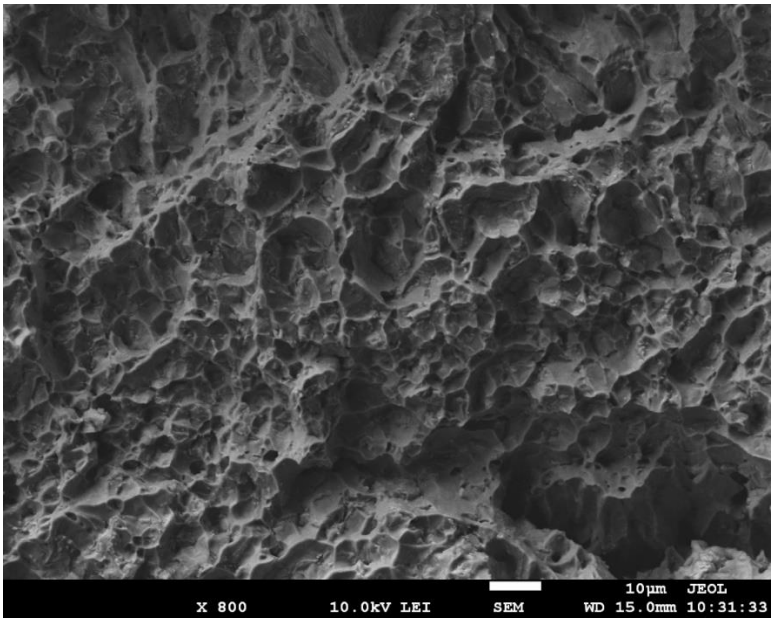

Figure 4. Fracture surface after tensile testing

Nanoindentation measurements were carried out in order to evaluate the mechanical properties of local zones in weld metal. The corresponding results are given in Tab. 3. Indents after testing are given in Fig. 5. Indents 1 and 2 are located in equiaxed zone. The measured nanoindentation hardness is lower than in remaining locations of weld metal. Nanoindentation hardness values increased in the direction towards weld centreline (indents 3 to 5).

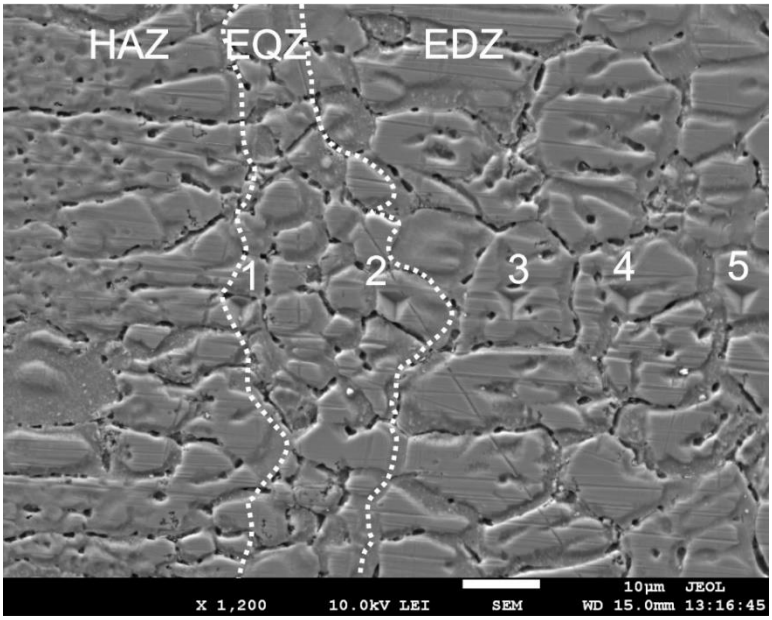

Figure 5. Distribution of indents across equiaxed non-dendritic zone and equiaxed dendritic zone of weld metal

Young's modulus and displacement at maximum load for indents 1 to 5 is given in Fig. 6. Lower Young's modulus and higher values of displacement at maximum load were recorded for equiaxed zone. Similar results were reported by Han et al. who investigated local softening in equiaxed zone of 2060-T8/2099-T83 aluminium lithium weld joints produced with laser beam welding [21].
The values of Young's modulus in the locations of indents 1 and 2 were 90 and 97 GPa, respectively. Contrary, displacement at maximum load for indents 1 and 2 reached higher values, 620 and 623 nm.

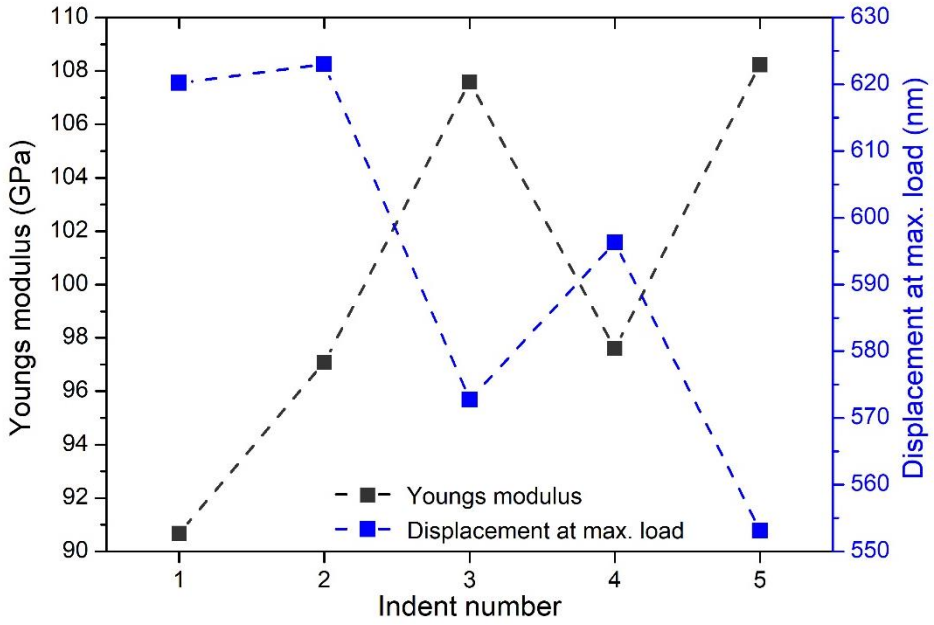

Figure 6. Young's modulus and displacement at maximum load for indents 1 to 5

Table 3. Results of nanoindentation hardness measured in various locations of weld metal

Zone in weld metal	Nanoindentation hardness (GPa)				
	1	2	3	4	5
EQZ	1.070	1.057			
EDZ			1.224	1.151	1.321

4 CONCLUSION

Microstructure and mechanical properties of AW2099 aluminium lithium alloy welded joints produced by electron beam welding were investigated. The major conclusions are as follows:

- the microstructure of weld metal is characterized by dendritic morphology. The matrix is formed with α-aluminium solid solution,
- produced weld joints consisted of heat affected zone, partially melted zone, equiaxed non-dendritic zone, columnar dendritic zone and equiaxed dendritic zone,

- character of grains changed from equiaxed to columnar dendrites in the direction to weld centreline, while equiaxed dendrites were observed in the weld centre,
- nanoindentation hardness values were lower for equiaxed zone in comparison to remaining parts of weld joint. Contrary, Young's modulus was higher for locations in mentioned zone,
- drop of weld joints strength was observed, i.e. the fracture occurred in the weld metal.

ACKNOWLEDGEMENT

This work was supported by the Slovak Research and Development Agency under the contract No. APVV-15-0337.

5 REFERENCES

[1] R. Xiao, X. Zhang, Problems and issues in laser beam welding of aluminum–lithium alloys, J. Mater. Process. Tech. 16 (2014) 166-175
[2] Ch. Gao, R. Gao, Y. Ma, Microstructure and mechanical properties of friction spot welding aluminium–lithium 2A97 alloy, Mater. Des. 83 (2015) 719-727
[3] B. Han, W. Tao, Y. Chen, H. Li, Double-sided laser beam welded T-joints for aluminum-lithium alloy aircraft fuselage panels: Effects of filler elements on microstructure and mechanical properties, Opt. Laser Technol. 93 (2017) 99-108
[4] H.-S. Lee, J.-H. Yoon, J.-T. Yoo, K. No, Friction stir welding process of aluminum-lithium alloy 2195, Procedia Eng. 149 (2016) 62-66
[5] Y. E. Ma, Z. C. Xia, R.R. Jiang, W. Y. Li, Effect of welding parameters on mechanical and fatigue properties of friction stir welded 2198 T8 aluminum–lithium alloy joints, Eng. Fract. Mech. 114 (2013) 1-11
[6] F. Zhang, J. Shen, X.-D. Yan, J.-L. Sun, X.-L. Sun, Y. Yang, Homogenization heat treatment of 2099 Al-Li alloy, Rare Met. 33 (2014) 28-36
[7] Y. Tao, D. R. Ni, B. L. Xiao, Z. Y. Ma, W. Wu, R. X. Zhang, Y. S. Zeng, Origin of unusual fracture in stirred zone for friction stir welded 2198-T8 Al-Li alloy joints, Mat. Sci. Eng., A 693 (2017) 1-13
[8] R. Rajan, P. Kah, B. Mvola, J. Martikainen, Trends in aluminium alloy development and their joining methods, Rev. Adv. Mater. Sci. 44 (2016) 383-397
[9] T. Dursun, C. Soutis, Recent developments in advanced aircraft aluminium alloys, Mater. Des. 56 (2014) 862–871
[10] M. Romios, R. Tiraschi, J. R. Ogren, H. W. Babel, Design of multistep aging treatments of 2099 (C458) Al-Li alloy, J. Mater. Eng. Perform. 14 (2005) 641-646
[11] G. Wang, Y. Zhao, Y. Hao, Friction stir welding of high-strength aerospace aluminium alloy and application in rocket tank manufacturing, Journal of Materials Science and Technology, 34, 2018, 73-91
[12] M. X. Milagre, N. V. Mogili, U. Donatus, R. A. R. Giorjão, M. Terada, J. V. S. Araujo, C. S. C. Machado, I. Costa, On the microstructure characterization of the AA2098-T351 alloy welded by FSW, Materials Characterization, 140, 2018, p. 233-246

[13] W. Y. Li, Q. Chu, X. W. Yang, J. J. Shen, A. Vairis, W. B. Wang, Microstructure and morphology evolution of probeless friction stir spot welded joints of aluminum alloy, Journal of Materials Processing Technology, 252, 2018, 69-80

[14] C. C. de Castro, A. H. Plaine, G. P. Dias, N. G. de Alcântara, J. F. dos Santos, Investigation of geometrical features on mechanical properties of AA2198 refill friction stir spot welds, Journal of Manufacturing Processes, 36, 2018, 330-339

[15] O. Hatamleh, I. V. Rivero, S. E. Swain, An investigation of the residual stress characterization and relaxation in peened friction stir welded aluminum–lithium alloy joints, Mater. Des. 30, 2009, p. 3367-3373

[16] X B. Fu, G. Qin, X. Meng, Y. Ji, Y. Zou, Zh. Lei : Microstructure and Mechanical Properties of Newly Developed Aluminum–Lithium Alloy 2A97 Welded by Fiber Laser. In Materials Science & Engineering 2014, vol. A617, p. 1–11

[17] D.C. Lin, G. X. Wang, T.S. Srivatsan: A Mechanism for the Formation of Equiaxed Grains in Welds of Aluminum-Lithium Alloy 2090. In Materials Science and Engineering 2003, vol. A351, p. 304-309

[18] A. H. Faraji, M. Moradi, M. Goodarzi, P. Colucci, C. Maletta: An Investigation on Capability of Hybrid Nd:YAG Laser-TIG Welding Technology for AA2198 Al-Li Alloy. Optics and Lasers in Engineering 2017, vol. 96, p. 1-6

[19] M. St. Weglowski, S. Blacha, A. Phillips, Electron beam welding - Techniques and trends - Review, Vacuum, 130, 2016, p. 72-92

[20] L. Cui, X. Li, D. He, L. Chen, Sh. Gong, Effect of Nd:YAG laser welding on microstructure and hardness of an Al–Li based alloy, Mater. Charact. 71, 2012, p. 95-102

[21] B. Han, Y. Chen, W. Tao, Zh. Lei, H. Li, Sh. Guo, P. Li, Nano-indentation investigation on the local softening of equi-axed zone in 2060-T8/2099-T83 aluminium-lithium alloys T-joints welded by double-sided laser beam welding, Journal of Alloys and Compounds, 756, 2018, p. 145-162